Thermal Science and Engineering 2024, 7(2), 8050.
https://doi.org/10.24294/tse.v7i2.8050

Article

Modified Cattaneo-Vernotte equation for heat transfer in solids

Victor L. Mironov

Institute for Physics of Microstructures, Russian Academy of Sciences, GSP-105, Nizhny Novgorod 603950, Russia; mironov@ipmras.ru

CITATION

Mironov VL. Modified Cattaneo-Vernotte equation for heat transfer in solids. Thermal Science and Engineering. 2024; 7(2): 8050. https://doi.org/10.24294/tse.v7i2.8050

ARTICLE INFO

Received: 18 April 2024
Accepted: 30 May 2024
Available online: 15 June 2024

Abstract: We propose a modified relation between heat flux and temperature gradient, which leads to a second-order equation describing the evolution of temperature in solids with finite rate of propagation. A comparison of the temperature field spreading in the framework of Fourier, Cattaneo-Vernotte (CV), and modified Cattaneo-Vernotte (MCV) equations is discussed. The comparative analysis of MCV and Fourier solutions is carried out on the example of a simple one-dimensional problem of plate cooling.

Keywords: Non-Fourier thermal conductivity; modified Cattaneo-Vernotte equation; microscale heat transfer

1. Introduction

In classical consideration, the process of heat transfer in solids is described by a phenomenological equation based on two assumptions [1]. The first is the continuity of heat propagation:

$$c\rho\frac{\partial\theta}{\partial t} + \nabla\cdot\mathbf{q} = 0 \tag{1}$$

where c is the specific heat capacity, ρ is the mass density, θ is the temperature, q is the vector of heat flux. The second assumption is Fourier's law, which establishes the relationship between heat flux and gradient of temperature

$$\mathbf{q} = -\kappa\nabla\theta \tag{2}$$

where κ is the thermal conductivity. Substitution (2) into Equation (1) gives the classical equation for the temperature evolution

$$\frac{\partial\theta}{\partial t} - \beta_q\Delta\theta = 0 \tag{3}$$

where $\beta_q = \kappa/c\rho$ is the thermal diffusivity, Δ is the Laplace operator.

The disadvantage of relation (2) is that it leads us to the equation of parabolic type (3), which describes the instantaneous propagation of heat [2–4]. However, this contradicts the physical nature of the heat transfer process.

To overcome the drawback in classical heat conduction, the different modifications of Fourier's law were proposed [3,4]. Among them, we can highlight "inertial" theories [4,5], nonlinear models [6,7], the dual-phase-lag approach [8], and more complicated models based on Oldroyd's upper-convected derivative [9,10] (which are used for the description of non-Fourier heat transfer in fluids [11–13]). Some historical considerations on the various hyperbolic heat equations can be found in [3,4,14,15].

In particular, the simple Fourier's law modification taking into account "inertia" of the heat transfer is formulated as follows [3–6]:

$$\tau_q \frac{\partial \mathbf{q}}{\partial t} + \mathbf{q} = -\kappa \nabla \theta \tag{4}$$

where τ_q is a relaxation time depending on material properties. When $\tau_q = 0$ the expression (4) is transformed to the Fourier's law (2). The relation (4) in combination with continuity condition (1) leads us to the wave equation of hyperbolic type

$$\tau_q \frac{\partial^2 \theta}{\partial t^2} + \frac{\partial \theta}{\partial t} - \beta_q \Delta \theta = 0 \tag{5}$$

which is widely discussed as Cattaneo-Vernotte (CV) equation [16–31].

Note that in the limiting case $\tau_q \to \infty$, $\kappa \to \infty$, β_q finite the equation (5) turns into a wave equation

$$\frac{\partial^2 \theta}{\partial t^2} - a^2 \Delta \theta = 0 \tag{6}$$

describing purely wave propagation of heat at a constant speed

$$a = \sqrt{\frac{\kappa}{c\rho\tau_q}} \tag{7}$$

The parabolic Fourier equation (3) and hyperbolic CV equation (5) describe the same stationary states, which are determined by the Laplace operator, but the dynamics of relaxation to these stationary states is different. However, eliminating the paradox of instantaneous heat propagation [4,20,21], the CV heat equation leads to other paradoxical results associated with interference of temperature waves, their reflection from the boundaries of the body, and the formation of shock heat waves [22–31]. Therefore, discussions about the applicability of the Fourier and CV equations continue [32,33].

Note also that the processes of diffusion and heat transfer have a similar nature [1,34], 34]. Therefore, the telegraph equations of hyperbolic type for diffusion are also discussed in the literature [35,36].

In this paper, we propose a modification of the CV approach to the description of heat transfer, which leads to the alternative equation and describes a different dynamics of heat transfer.

2. Comparison of Fourier equation and Cattaneo-Vernotte equation

Let us compare Fourier and CV equations in detail. The Equation (4) introduces a very important parameter τ_q that describes the time scale of heat relaxation and allows one to determine the characteristic rate of heat propagation as

$$s_q^2 = \frac{\beta_q}{\tau_q} \tag{8}$$

and the characteristic spatial scale of heat diffusion as

$$l_q = \sqrt{\beta_q \tau_q} = s_q \tau_q \tag{9}$$

This allows one to rewrite Fourier and CV equations in the similar form

$$\frac{1}{\tau_q}\frac{\partial \theta}{\partial t} - s_q^2 \Delta \theta = 0 \tag{10}$$

$$\frac{\partial^2 \theta}{\partial t^2} + \frac{1}{\tau_q}\frac{\partial \theta}{\partial t} - s_q^2 \Delta \theta = 0 \tag{11}$$

The Equations (10) and (11) admit the solutions in the form of plane waves

$$\theta = A\exp\left(i\omega t + i\left(\boldsymbol{k}\cdot\boldsymbol{r}\right)\right) \tag{12}$$

where ω is the frequency, $k$is the wave vector. The dispersion relation for parabolic Fourier Equation (10) is

$$\omega = i\tau_q s_q^2 k^2 \tag{13}$$

where k is the wave number ($k = |\boldsymbol{k}|$). In this relation, the frequency is an imaginary quantity. Thus, the solutions of the Fourier equation are spatial harmonics decaying with time. The damping factor is

$$i\omega = -\tau_q s_q^2 k^2 \tag{14}$$

The dependence of the decrement (14) on the wave number is shown in**Figure 1**.

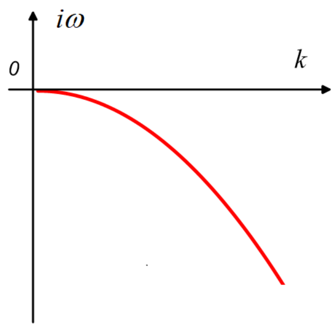

Figure 1. The schematic plot of dispersion dependence for parabolic Fourier equation.

Also, we can introduce the analog of group speed, which is the imaginary value

$$i\,v_F = i\frac{d\omega}{dk} = -2\tau_q s_q^2 k. \tag{15}$$

This value tends to infinity ($iv_F \to -\infty$) when $k \to \infty$, that is the reason of the infinitely fast scattering of shortwave harmonics.

On the other hand, the dispersion relation for hyperbolic CV Equation (11) is

$$\omega^2 + \frac{i\omega}{\tau_q} - s_q^2 k^2 = 0 \tag{16}$$

From (16) we obtain

$$\omega = i\,\frac{1 \pm \sqrt{1 - 4l_q^2 k^2}}{2\tau_q} \tag{17}$$

The behavior of spatial harmonics essentially depends on their wave number. In the region of wave numbers $k < k^*$ (where $k^* = \frac{1}{2l_q}$), solutions of CV equation also represent damped spatial harmonics. The damping factor is

$$i\omega = -\frac{1 \pm \sqrt{1 - 4l_q^2 k^2}}{2\tau_q} \tag{18}$$

Dispersion dependence (18) is shown in **Figure 2**.

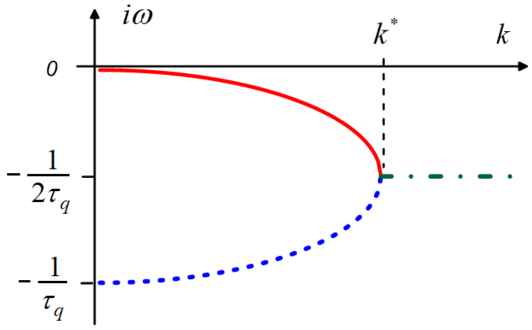

Figure 2. The schematic plot of decrement for hyperbolic CV equation. The solid curve corresponds to the "–" sign in expression (18), the dotted curve corresponds to the "+" sign. The dash-dotted line in the region $k > k^*$ represents the decrement in expression (19).

In the region $k < k^*$, the decrement has two branches (shown by solid and dotted lines in **Figure 2**) in accordance with the signs in expression (18). At small k on the upper branch of the dispersion curve, the decrement is $i\omega \approx -\tau_q s_q^2 k^2$, that coincides with the decrement of the Fourier Equation (14).

In the region $k > k^*$, the dispersion dependence (18) has both imaginary and real parts

$$\omega = i\frac{1}{2\tau_q} \pm \frac{\sqrt{4l_q^2 k^2 - 1}}{2\tau_q}. \tag{19}$$

The damping factor in this region of wave numbers is equal to

$$i\omega = -\frac{1}{2\tau_q} \tag{20}$$

It is shown by the dot-dashed line in **Figure 2**. The real part of the dispersion relation (19) is shown in **Figure 3**.

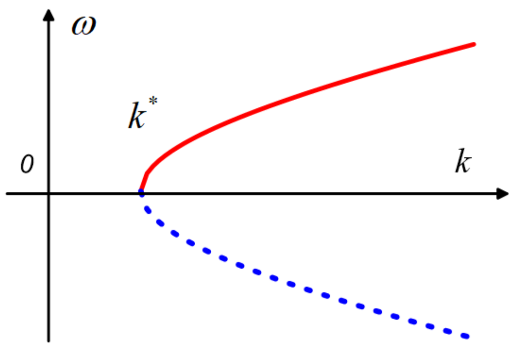

Figure 3. The schematic plot of the real part of dispersion curves for CV equation.

The region of wave numbers $k > k^*$ corresponds to the spatial harmonics propagating in the form of traveling waves. In this region CV equation has the real group velocity.

$$v_{CV} = \frac{d\omega}{dk} = \frac{2l_q^2}{\tau_q}\frac{k}{\sqrt{4l_q^2k^2 - 1}} \tag{21}$$

This value tends to be constant s_q ($v_{CV} \to s_q$) when $k \to \infty$. However, the group velocity of harmonics with k near k^* still tends to an infinite value. A more extended spectral analysis of the CV equation can be found in [37].

3. Modified Cattaneo-Vernotte equation of heat transfer

Evidently, the hyperbolic heat equation is a consequence of the concept of "inertia" for heat flow. However, this concept raises doubts since the macroscopic transfer of heat is associated not with their directed motion but with chaotic vibrations of atoms in the crystal lattice. Here we propose the modification of CV condition (4) that leads to an alternative equation describing different dynamics of heat propagation.

Let us first analyze the CV modification of Fourier's law. It assumes the lagging response in time between the heat flux vector and the temperature gradient. Mathematically, this can be expressed as:

$$\mathbf{q}(\boldsymbol{r}, t + \tau_q) = -\kappa\nabla\theta(\boldsymbol{r}, t) \tag{22}$$

where τ_q is the phase-lag in time. Expression (22) shows that the temperature gradient established at time t is defined by heat flux vector at a later time $t + \tau_q$. Assuming the smallness of the parameter τ_q, we can expand the left side of equation (22) into a Taylor series:

$$\mathbf{q}(\boldsymbol{r}, t + \tau_q) = \mathbf{q}(\boldsymbol{r}, t) + \tau_q\frac{\partial\mathbf{q}(\boldsymbol{r}, t)}{\partial t} + O(\tau_q^2) \tag{23}$$

Then, keeping only the first-order term in τ_q and substituted into (22), we arrive at the expression (4), where the term $\tau_q\partial\mathbf{q}/\partial t$ describes the acceleration of heat propagation.

However, it is natural to assume that the temperature gradient at a given point depends not on the heat flow in the future $t + \tau_q$, but on the flow at the previous moment in time $t - \tau_q$. This is expressed by the following condition:

$$\mathbf{q}(\boldsymbol{r}, t - \tau_q) = -\kappa\nabla\theta(\boldsymbol{r}, t) \tag{24}$$

Expanding the left side (24) into a Taylor series we get:

$$\mathbf{q}(\boldsymbol{r}, t - \tau_q) = \mathbf{q}(\boldsymbol{r}, t) - \tau_q\frac{\partial\mathbf{q}(\boldsymbol{r}, t)}{\partial t} + O(\tau_q^2) \tag{25}$$

Here the term $-\tau_q\partial\mathbf{q}/\partial t$ describes the slowing down of heat propagation. Thus, in combination with the continuity Equation (1), we arrive at the following modified system describing heat transfer:

$$c\rho\frac{\partial\theta}{\partial t} + \boldsymbol{\nabla}\cdot\mathbf{q} = 0 \tag{26}$$

$$-\tau_q\frac{\partial\mathbf{q}}{\partial t} + \mathbf{q} + \kappa\nabla\theta = 0 \tag{27}$$

The system (26) – (27) is equivalent to the following MCV equation for the temperature field:

$$\frac{\partial^2\theta}{\partial t^2}-\frac{1}{\tau_q}\frac{\partial\theta}{\partial t}+s_q^2\Delta\theta=0 \tag{28}$$

Note that the stationary state of MCV Equation (28) is the same as for the Fourier (3) and CV (5) equations, but the time evolution of temperature is different.

Let us analyze the consequences of the proposed modification. Assuming harmonic solutions (12), we have the following dispersion relation for the MCV equation:

$$\omega^2+i\frac{1}{\tau_q}\omega+s_q^2k^2=0 \tag{29}$$

From (29) we have two roots:

$$i\omega=\frac{1\pm\sqrt{1+4\tau_q^2s_q^2k^2}}{2\tau_q} \tag{30}$$

The schematic plots of dispersion curves (30) are represented in **Figure 4**.

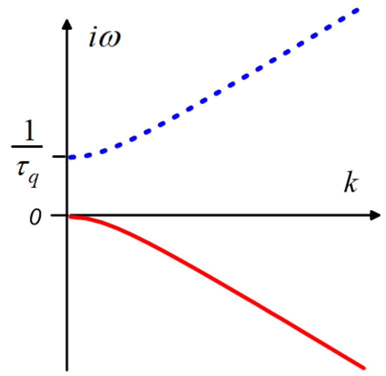

Figure 4. The schematic plots of dispersion curves for MCV equation.

The upper branch of dispersion curve corresponds to:

$$i\omega=\frac{1+\sqrt{1+4\tau_q^2s_q^2k^2}}{2\tau_q} \tag{31}$$

and describes the solutions growing in time that contradict the physical picture of the heat transfer process and are a consequence of the violation of the causality principle [38]. However, on the other hand, the solutions corresponding to the lower branch of the dispersion characteristic with describe damped in time spatial harmonics and can be used to describe the process of heat propagation.

$$i\omega=\frac{1-\sqrt{1+4\tau_q^2s_q^2k^2}}{2\tau_q} \tag{32}$$

4. Comparison of Fourier equation and modified Cattaneo-Vernotte equation

Let us compare Fourier and MCV equations. We write these equations in the similar form:

$$\frac{1}{\tau_q}\frac{\partial\theta}{\partial t}-s_q^2\Delta\theta=0 \tag{33}$$

$$-\frac{\partial^2\theta}{\partial t^2}+\frac{1}{\tau_q}\frac{\partial\theta}{\partial t}-s_q^2\Delta\theta=0 \tag{34}$$

The dispersion relation for Fourier Equation (33) is

$$i\omega=-\tau_q s_q^2 k^2 \tag{35}$$

The dispersion relation for MCV Equation (34) is

$$i\omega=\frac{1-\sqrt{1+4\tau_q^2 s_q^2 k^2}}{2\tau_q}. \tag{36}$$

The schematic plots of (35) and (36) are represented in **Figure 5**.

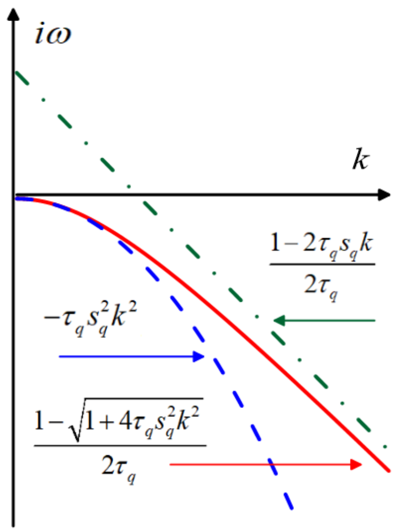

Figure 5. The schematic plot of dispersion curves for Fourier (dashed blue line) and MCV (solid red line) equations. The asymptote (37) is shown by dot-dashed line.

In the region of small k the dependence (36) coincides with dependence (35), while at $k\to\infty$it tends to the asymptote

$$i\omega=\frac{1-2\tau_q s_q k}{2\tau_q} \tag{37}$$

The analog of group speed for MCV equation is

$$i\,v_{MCV}=i\frac{d\omega}{dk}=-\frac{2\tau_q s_q^2 k}{\sqrt{1+4\tau_q^2 s_q^2 k^2}}. \tag{38}$$

This quantity tends to be constant $-s_q$at $k\to\infty$. On the other hand, taking into account (12) the analog of group speed for Fourier equation is

$$i\,v_F=i\frac{d\omega}{dk}=-2\tau_q s_q^2 k. \tag{39}$$

This quantity tends to infinity at $k \to \infty$.

4.1. The plate cooling

As an example, let us consider the one-dimensional problem of cooling a plate with thickness $2l$ uniformly heated to a temperature θ_0 and with zero temperature at the boundaries $x = \pm l$. In this case we have natural spatial scale l and we introduce new dimensionless variables $\tilde{t} = t/\tau_q$ and $\tilde{x} = x/l$. Then the Fourier equation is represented as

$$\frac{\partial \theta}{\partial \tilde{t}} - \lambda^2 \frac{\partial^2 \theta}{\partial \tilde{x}^2} = 0 \tag{40}$$

while MCV equation is

$$\frac{\partial^2 \theta}{\partial \tilde{t}^2} - \frac{\partial \theta}{\partial \tilde{t}} + \lambda^2 \frac{\partial^2 \theta}{\partial \tilde{x}^2} = 0 \tag{41}$$

where $\lambda = l_q/l$ is the ratio of the diffusion length to half of the plate thickness. Corresponding dispersion relations are

$$i\omega = -\lambda^2 k^2 \tag{42}$$

and

$$i\omega = \frac{1 - \sqrt{1 + 4\lambda^2 k^2}}{2}. \tag{43}$$

The solution to this problem in the frame of Fourier equation (40) is expressed by the following Fourier series [1]:

$$\theta_F = \frac{4\theta_0}{\pi} \sum_{m=0}^{\infty} \frac{(-1)^m}{(2m+1)} \cos\left[\frac{(2m+1)\pi}{2}\tilde{x}\right] \exp\left[-\frac{\lambda^2 (2m+1)^2 \pi^2}{4}\tilde{t}\right] \tag{44}$$

with decrement of temperature damping

$$d_{F\,m} = \frac{\lambda^2 (2m+1)^2 \pi^2}{4}. \tag{45}$$

On the other hand, the solution to this problem in the case of MCV equation (41) is expressed by the following series:

$$\theta_M = \frac{4\theta_0}{\pi} \sum_{m=0}^{\infty} \frac{(-1)^m}{(2m+1)} \cos\left[\frac{(2m+1)\pi}{2}\tilde{x}\right] \exp\left[\frac{1 - \sqrt{1 + \lambda^2 (2m+1)^2 \pi^2}}{2}\tilde{t}\right] \tag{46}$$

with damping parameter

$$d_{M\,m} = \frac{1 - \sqrt{1 + \lambda^2 (2m+1)^2 \pi^2}}{2}. \tag{47}$$

Thus, comparing damping parameters in (45) and (47) one can see that in case of MCV equation the higher harmonics decay more slowly than in case of Fourier equation in accordance with dispersion dependences (42) and (43).

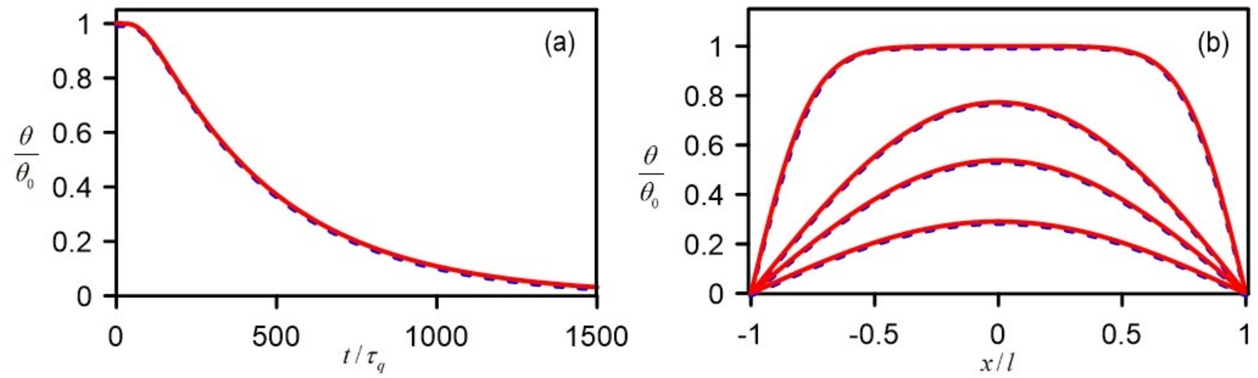

Figure 6. The process of cooling the thick plate with $l > l_q$ ($\lambda^2 = 0.01$). **(a)** Time dependences of temperature at the point $\tilde{x} = 0$; **(b)** Temperature profiles at different time ($\tilde{t} = 20, 200, 350, 600$). The solutions of Fourier equation are indicated by dashed blue lines. Solutions of MCV equation are shown by solid red lines.

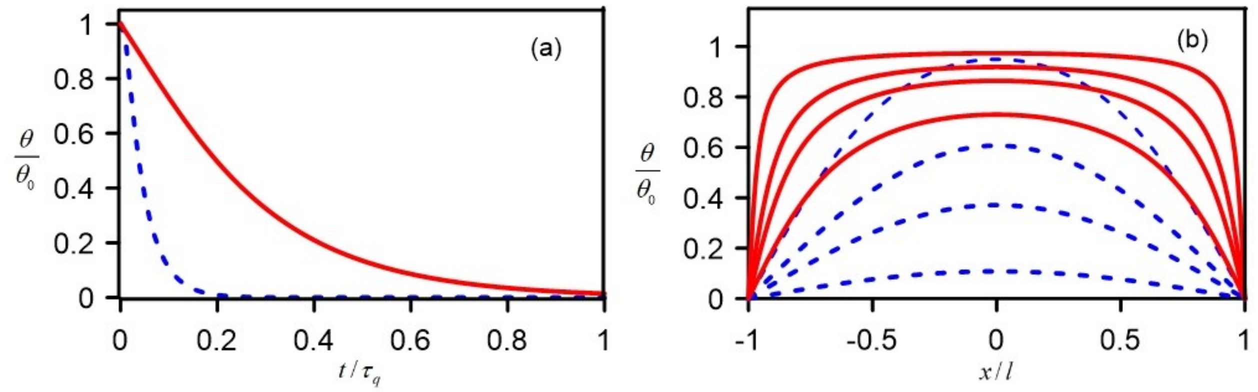

Figure 7. The process of cooling the thin plate with $l < l_q$ ($\lambda^2 = 10$). **(a)** Time dependences of temperature at the point $\tilde{x} = 0$; **(b)** Temperature distributions at different time ($\tilde{t} = 0.01, 0.03, 0.05, 0.1$). The solutions of Fourier equation are indicated by dashed blue lines. Solutions of MCV equation are shown by solid red lines.

The results of numerical calculations for the plates with different thicknesses are represented in **Figures 6** and **7**. It is seen that in the case of thick plates ($l > l_q$) the solution of the MCV equation (red solid curves in **Figure 6a,b**) coincides with the solution of the Fourier equation (blue dashed curves in **Figure 6a,b**). However, for thin plates ($l < l_q$) the solution to the Fourier equation demonstrates a rapid decrease in temperature gradients and faster cooling of the plate (blue dashed curves in **Figure 7a,b**) than in the case of the solution described by the MCV equation (red solid curves in **Figure 7a,b**).

To clarify the time evolution of Fourier and MCV solutions, we analyze the behavior of zero harmonics. Let us consider the cooling a plate (thickness $2l$) with $\theta_0 \cos(\pi x/2l)$ initial temperature and with zero temperature at the boundaries $x = \pm l$. In this case,

$$\theta_F = \theta_0 \cos\left(\frac{\pi}{2}\tilde{x}\right)\exp\left(-\frac{\lambda^2\pi^2}{4}\tilde{t}\right), \tag{48}$$

and

$$\theta_M = \theta_0 \cos\left(\frac{\pi}{2}\tilde{x}\right)\exp\left(\frac{1-\sqrt{1+\lambda^2\pi^2}}{2}\tilde{t}\right). \tag{49}$$

The dependence of the ratio of damping parameters d_M/d_F as the function of λ is represented in **Figure 8**.

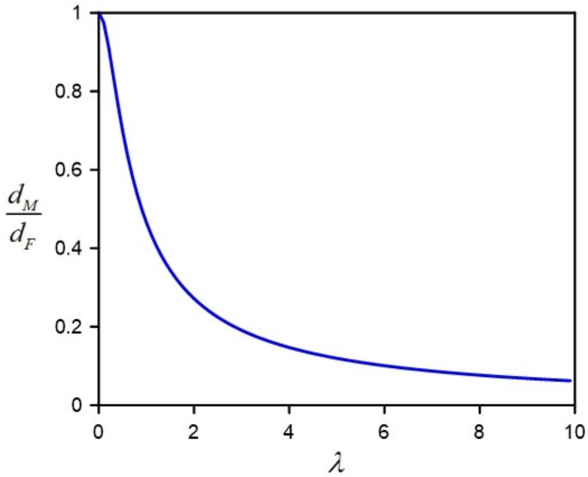

Figure 8. The dependence of damping parameters ratio d_M/d_F on the parameter λ.

For thick plates when $\lambda^2\pi^2 \ll 1$ we have

$$d_M \approx -\frac{\lambda^2\pi^2}{4} = d_F \tag{50}$$

and time behavior of Fourier and MCV solutions is practically the same. The temperature profiles at different times and the dependence of temperature at the central point of the plate on time are shown in **Figure 9**.

In opposite case of thin plate when $\lambda^2\pi^2 \gg 1$ we have

$$d_M \approx -\frac{\lambda\pi}{2} < d_F \tag{51}$$

and MCV equation predicts slower cooling than Fourier equation. The corresponding temperature profiles and time dependences are shown in **Figure 10**.

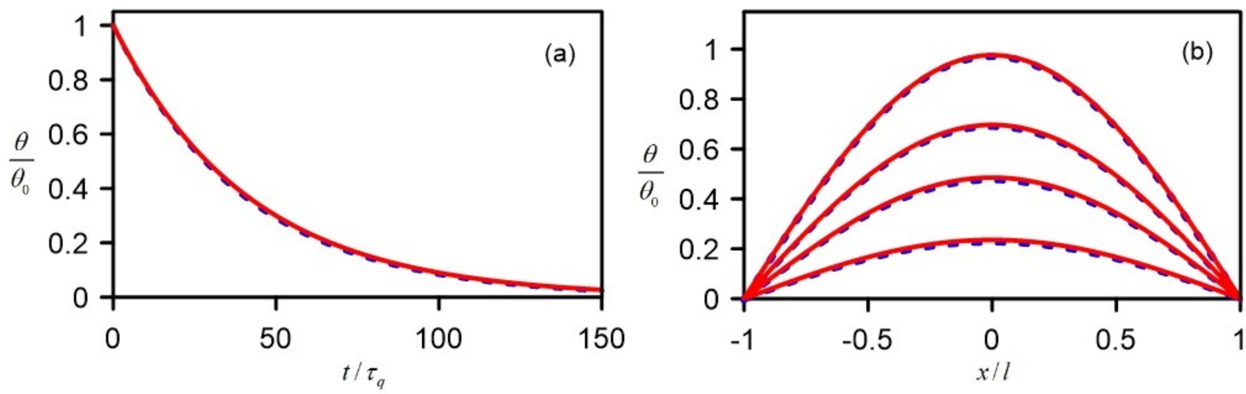

Figure 9. The process of cooling the thick plate with $l > l_q$ ($\lambda^2 = 0.01$). **(a)** Time dependences of temperature at the point $\tilde{x} = 0$; **(b)** Temperature distributions at different time ($\tilde{t} = 1, 15, 30, 60$). The solutions of Fourier equation are indicated by dashed blue lines. Solutions of MCV equation are shown by solid red lines.

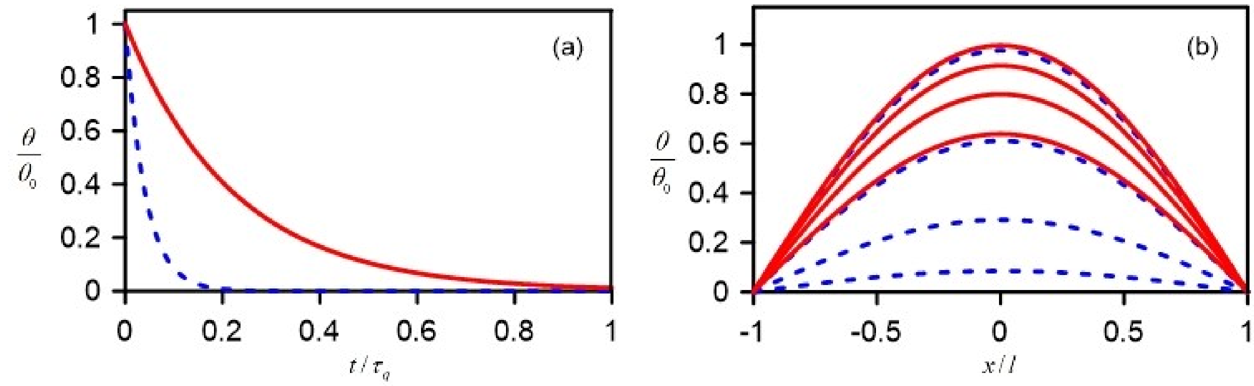

Figure 10. The process of cooling the thick plate with $l > l_q$ ($\lambda^2 = 0.01$). **(a)** Time dependences of temperature at the point $\tilde{x} = 0$; **(b)** Temperature distributions at different time ($\tilde{t} = 0.001, 0.02, 0.05, 0.1$). The solutions of Fourier equation are indicated by dashed blue lines. Solutions of MCV equation are shown by solid red lines.

Thus, it is seen that the differences between solutions of Fourier and MCV equations are noticeable only at small spatial scales, when the plate thickness is less than the diffusion length. This approach can be applied to describe the non-Fourier thermal effects at micro scales [8].

5. Conclusion

We propose an alternative relationship between heat flux and temperature gradient, which leads us to the MCV equation describing the evolution of temperature with a finite rate. Solutions of MCV equations have the same spatial temperature distributions as in the case of Fourier and CV equations but describe a different dynamics of heat transfer process. The peculiarities of MCV solutions and their comparison with Fourier solutions have been analyzed on the example of the simple problem of plate cooling. It was shown that on large spatial scales, when the plate thickness is greater than the thermal diffusion length, the differences between the solutions of MCV and Fourier equations are insignificant. However, in the case when the plate thickness is less than the diffusion length, the MCV equation predicts a slower cooling in accordance with a finite heat transfer rate.

Thus, it has been shown that the MCV equation provides the finite rate of transfer processes, but it does not have the disadvantages of a CV equation, which predicts many paradoxical results associated with the possible propagation of heat in the form of real harmonic waves. The same approach can be applied to describe the diffusion processes in solids.

Acknowledgments: The author is grateful to the reviewers for their very useful and stimulating comments and suggestions.

Conflict of interest: The author declares no conflict of interest.

References

1. Carslow HS, Jaeger JC. Conduction of heat in solids. Oxford University Press, Oxford, UK, 1959.
2. Christov CI, Jordan PM. Heat Conduction Paradox Involving Second-Sound Propagation in Moving Media. Physical Review Letters. 2005; 94(15). doi: 10.1103/physrevlett.94.154301

3. Chandrasekharaiah DS. Hyperbolic Thermoelasticity: A Review of Recent Literature. Applied Mechanics Reviews. 1998; 51(12): 705-729. doi: 10.1115/1.3098984
4. Joseph DD, Preziosi L. Heat waves. Reviews of Modern Physics. 1989; 61(1): 41-73. doi: 10.1103/revmodphys.61.41
5. Green AE, Naghdi PM. A re-examination of the basic postulates of thermomechanics. In: Proceedings of the Royal Society of London Series A: Mathematical and Physical Sciences. 1991; 432(1885): 171-194. doi: 10.1098/rspa.1991.0012
6. Cimmelli VA, Kosinski W, Saxton K. Modified Fourier law: Comparison of two approaches, Archives of Mechanics. 1992; 44, 409-415.
7. Ignaczak J. Soliton-like solutions in a nonlinear dynamic coupled thermoelasticity. Journal of Thermal Stresses. 1990; 13(1): 73-98. doi: 10.1080/01495739008927025
8. Tzou DY. A Unified Field Approach for Heat Conduction From Macro- to Micro-Scales. Journal of Heat Transfer. 1995; 117(1): 8-16. doi: 10.1115/1.2822329
9. Christov CI. On frame indifferent formulation of the Maxwell–Cattaneo model of finite-speed heat conduction. Mechanics Research Communications. 2009; 36(4): 481-486. doi: 10.1016/j.mechrescom.2008.11.003
10. Oldroyd JG. On the formulation of rheological equations of state. In: Proceedings of the Royal Society of London Series A Mathematical and Physical Sciences. 1950; 200(1063): 523-541. doi: 10.1098/rspa.1950.0035
11. Khan U, Ahmad S, Hayyat A, et al. On the Cattaneo–Christov Heat Flux Model and OHAM Analysis for Three Different Types of Nanofluids. Applied Sciences. 2020; 10(3): 886. doi: 10.3390/app10030886
12. Jafarimoghaddam A, Turkyilmazoglu M, Pop I. Threshold for the generalized Non-Fourier heat flux model: Universal closed form analytic solution. International Communications in Heat and Mass Transfer. 2021; 123: 105204. doi: 10.1016/j.icheatmasstransfer.2021.105204
13. Turkyilmazoglu M. Heat Transfer Enhancement Feature of the Non-Fourier Cattaneo–Christov Heat Flux Model. Journal of Heat Transfer. 2021; 143(9). doi: 10.1115/1.4051671
14. Joseph DD, Preziosi L. Addendum to the paper “Heat waves” [Rev. Mod. Phys. 61, 41 (1989)]. Reviews of Modern Physics. 1990; 62(2): 375-391. doi: 10.1103/revmodphys.62.375
15. Sobolev SL. On hyperbolic heat-mass transfer equation. International Journal of Heat and Mass Transfer. 2018; 122: 629-630. doi: 10.1016/j.ijheatmasstransfer.2018.02.022
16. Cattaneo C.On the Calculation of Certain Potentials and Their Intervention in the Solving of Particular Harmonic Problems (Italian). In: Proceedings of the Mathematical and Physical Seminar of the University of Modena and Reggio Emilia, 1948; 3, 29-45.
17. Cattaneo C. A form of heat equation which eliminates the paradox of instantaneous propagation. Comptes Rendus de l'Academie des Sciences. 1958; 247, 431-433.
18. Vernotte P. Paradoxes in the continuous theory of the heat equation. Comptes Rendus de l'Academie des Sciences. 1958; 246, 3154-3155.
19. Vernotte P. The true heat equation. Comptes Rendus de l'Academie des Sciences. 1958; 247, 2103.
20. O¨zis¸ik MN, Tzou DY. On the Wave Theory in Heat Conduction. Journal of Heat Transfer. 1994; 116(3): 526-535. doi: 10.1115/1.2910903
21. Mandrusiak GD. Analysis of Non-Fourier Conduction Waves from a Reciprocating Heat Source. Journal of Thermophysics and Heat Transfer. 1997; 11(1): 82-89. doi: 10.2514/2.6204
22. Xu M, Wang L. Thermal oscillation and resonance in dual-phase-lagging heat conduction, International Journal of Heat and Mass Transfer. 2002; 45(5), 1055-1061.
23. Barletta A, Zanchini E. Hyperbolic heat conduction and thermal resonances in a cylindrical solid carrying a steady periodic electric field, International Journal of Heat and Mass Transfer. 1996; 39 (6), 1307-1315.
24. Özisik MN, Vick B. Propagation and reflection of thermal waves in a finite medium, International Journal of Heat and Mass Transfer. 1984; 27 (10), 1845-1854.
25. Tzou DY. Shock wave formation around a moving heat source in a solid with finite speed of heat propagation, International Journal of Heat and Mass Transfer. 1989; 32 (10), 1979-1987.
26. Carey GF, Tsai M. Hyperbolic heat transfer with reflection. Numerical Heat Transfer. 1982; 5(3): 309-327. doi: 10.1080/10407788208913451
27. Kheibari AK, Jafari M, Nazari MB. Propagation of heat wave in composite cylinder using Cattaneo- Vernotte theory. International Journal of Heat and Mass Transfer. 2020; 160: 120208. doi: 10.1016/j.ijheatmasstransfer.2020.120208

28. van der Merwe AJ, van Rensburg NFJ, Sieberhagen RH. Comparing the dual phase lag, Cattaneo-Vernotte and Fourier heat conduction models using modal analysis. Applied Mathematics and Computation. 2021; 396: 125934. doi: 10.1016/j.amc.2020.125934
29. Nosko O. Perfect thermal contact of hyperbolic conduction semispaces with an interfacial heat source. International Journal of Heat and Mass Transfer. 2021; 164: 120541. doi: 10.1016/j.ijheatmasstransfer.2020.120541
30. Yuvaraj R, Senthil Kumar D. Numerical simulation of thermal wave propagation and collision in thin film using finite element solution. Journal of Thermal Analysis and Calorimetry. 2020; 142(6): 2351-2369. doi: 10.1007/s10973-020-09346-y
31. Kovács R, Rogolino P. Numerical treatment of nonlinear Fourier and Maxwell-Cattaneo-Vernotte heat transport equations. International Journal of Heat and Mass Transfer. 2020; 150: 119281. doi: 10.1016/j.ijheatmasstransfer.2019.119281
32. Auriault JL. The paradox of fourier heat equation: A theoretical refutation. International Journal of Engineering Science. 2017; 118: 82-88. doi: 10.1016/j.ijengsci.2017.06.006
33. Maillet D. A review of the models using the Cattaneo and Vernotte hyperbolic heat equation and their experimental validation. International Journal of Thermal Sciences. 2019; 139: 424-432. doi: 10.1016/j.ijthermalsci.2019.02.021
34. Mehrer H. Diffusion in Solids. Springer Berlin Heidelberg; 2007. doi: 10.1007/978-3-540-71488-0
35. Litvinenko YE, Schlickeiser R. The telegraph equation for cosmic-ray transport with weak adiabatic focusing. Astronomy & Astrophysics. 2013; 554: A59. doi: 10.1051/0004-6361/201321327
36. Tautz RC, Lerche I. Application of the three-dimensional telegraph equation to cosmic-ray transport. Research in Astronomy and Astrophysics. 2016; 16(10): 162. doi: 10.1088/1674-4527/16/10/162
37. Zhang D, Ostoja-Starzewski M. Telegraph equation: two types of harmonic waves, a discontinuity wave, and a spectral finite element. Acta Mechanica. 2019; 230(5): 1725-1743. doi: 10.1007/s00707-018-2356-3
38. Sommerfeld A. Introduction to Partial Differential Equations. Partial Differential Equations in Physics. 1949; 32-62. doi: 10.1016/b978-0-12-654658-3.50006-9